STUDY OF THREE-DIMENSIONAL ON-LINE PATH PLANNING FOR UAV BASED ON PYTHAGOREAN HODOGRAPH CURVE

ZHANG Yi, YANG Xiu-xia, ZHOU Wei-wei and ZHAO He-wei
Department of Control Engineering
Naval Aeronautical and Astronautical University
Yantai, China
Emails: yangxiuxia@126.com

Submitted: Apr. 10, 2015 ***Accepted: July 21, 2015*** ***Published: Sep. 1, 2015***

Abstract- For the demand of the UAV autonomous path planning in dynamic thread environment, the three-dimensional path planning algorithm on-line of UAV based on Pythagorean Hodograph (PH) curve is put forward. According to the UAV's current flight state such as location and speed, and the interrupt point or the target's state, a flyable path with continuous curvature is planed out online. The roles of the key parameters are analyzed and the range of the values are given. On this basis, the distribution estimation algorithm is used to optimize the selection of path parameters, which avoid the blindness iterative process and consider the kinematics constraints such as the curvature, torsion and climbing angle. The multiple UAVs' three dimensional path planning in dynamic environment are tested. Simulation results prove the validity and practicability of the algorithm.

Index terms*:* UAV, PH curve, three-dimensional path planning.

I. INTRODUCTION

When UAV executes missions in the complex environment, it is required to be able to adapt to the environment and can automatically plan flyable path online under encountering obstacles. As the motion of the UAV's platform is high-speed in real time, the independent control system of platform must operate and compute in real time. As a result, lots of offline methods which are time-consuming and have large calculation quantity, such as some intelligent optimization algorithms[1], aren't applied directly.

Some scholars put forward that the curve can be applied to path planning directly, which is easy to trace, for example, Dubins curve is applied to multiple UAVs' path planning which Shanmugavel, M.,et al[2] propose. Dubins path is composed by segmental arc and straight line, and from the perspective of the theory of differential geometry, in order to get a smooth flight path, the first two derivative of the path exists at least, that is, the curvature of the curve is continuous. Dubins path is the curve of C_1 type, but not the curve of C_2 type. Literature [3] gives the method of obtaining the path of continuous curvature by Clothoids curve. And the curvature changes linearly along the path, but the length of the path is not easy to generate closed solution. K.G. Jolly[4] applies the Bezier curve to the mobile robot's path planning. Literature [5] plans the parafoil terminal guidance path using the Bezier curve. Literature [6] plans the three dimensional flight path for UAV by using the Bezier curve of seven order, which considers climbing angle, curvature, torsion and so on system performance constraints. At present, Pythagorean Hodograph (PH) curve is widely used in aircrafts' on-line path planning[7-10], and the planning path is a path of C_2 type which the curvature is continuous. In contrast to other curves, it has a lot of advantages. The overall curvature of the curve is small. The length, curvature and bending energy of the curve can be calculated in closed form. The position and direction of the start point and end point are directly used in boundary conditions. The length and curvature can be coordinated easily. The generation of PH curve can be based on the Bezier spline curve, so it also has the advantages of the Bezier curve. Among them, the quintic PH curve is the lowest order PH curve which contains inflection points. Inflection points make the flight path have better flexibility, and to plan flight path better.

The generation method of PH curve path is given in literature [7]. Considering the performance constraints, such as curvature constraint, torsion constraint and so on, the length of beginning and

ending tangent vector on the PH control points should increase when the generated flight path doesn't meet the requirements of constraints, and the length of flight path will increase at the same time. But the optimal coordination of the two parameters' selection isn't studied in literature, and the path planning only considers the slow-moving or static obstacles on the plane and doesn't consider in three-dimensional path planning. Literature [9] adopts RRT (Rapid-Extended Random Tree) technology to find the path points, and then the two-dimensional path of PH curve is generated which uses multiple Pythagorean Hodograph (PH) curves to connect spanning trees. Literature [8] uses the PH curve to conduct three-dimensional path planning under the conditions of maximum curvature, torsion and climbing angle. The method of control parameters' iteration, according to the climbing angle, is given in this literature, and it makes the path flyable by increasing the length of the tangent vector on control points for the curves that don't satisfy the performance indicators. Essentially, this method belongs to fixed step iteration method, and does not consider the mutual influence of the tangent vectors on the starting and ending points. Besides, the iteration step-size is too long and the method easily makes the planning path too long.

In this paper, considering the dynamic performance constraints of curvature, torsion and climbing angle at the time of flying, the quintic PH curve is adopted to conduct three-dimensional path planning and the continuous curvature path can be planned online based on the current flight states of UAV and the motion information of target point. The value ranges of parameters are given by analyzing the influence of important planning parameters on the path's generation and combining with literature [8]. On this basis, Estimation of Distribution Algorithms[11] is adopted to the optimization and selection of path's parameters that is suitable for solving the problem, which avoids the blindness of parameters' selection in literature. In the process of obstacle avoidance, if the relative movement trend between the UAVs and the objects can be considered, then better effects of collision avoidance can be got. There have been many attempts to apply kinematic methods to solve the problem of collision detection. In literature [12-16], the notion of velocity obstacle is introduced for collision detection and resolution. In literature [12], collision cones(CC) is used for three-dimensional conflict resolution and the plane reduced-order[12] obstacle avoidance is adopted to conduct autonomous obstacle avoidance online based on the theory of speed-obstacle method. In this paper, the speed-obstacle method based on the

dimensional reduction is used to the obstacle avoidance, and the path can be re-planned by giving the insertion point of obstacle avoidance.

II. DESCRIPTION OF 3-D ONLINE FLYABLE PATH PLANNING PROBLEM

a. Constraints and performance metrics of 3-D PH path planning

It is assumed that the starting position $p_s(x_s, y_s, z_s)$, starting angle (θ_s, ϕ_s), ending position $p_f(x_f, y_f, z_f)$ and ending angle (θ_f, ϕ_f) are known, that is, the positions and poses of starting and ending points are $pose_s(x_s, y_s, z_s, \theta_s, \phi_s)$ and $pose_f(x_f, y_f, z_f, \theta_f, \phi_f)$ respectively. Among them, θ is the climbing angle and ϕ is the head angle. The UAV path is defined as $r(t) = [x(t), y(t), z(t)]$, and its curvature and torsion are κ and τ respectively. The formula of path planning can be expressed as: $pose_s(x_s, y_s, z_s, \theta_s, \phi_s) \xrightarrow{r(t)} pose_f(x_f, y_f, z_f, \theta_f, \phi_f)$, the picture representation of this problem is shown in figure 1. When the UAV detects the obstacle, the path interruption point should be calculated, and the path will be re-planned between the interruption point and the ending point.

Figure 1. 3-D Path Planning

Planning path $r(t)$, the following constraints need to be satisfied,

(1) Curvature constraint

$$|\kappa(t)| \le \kappa_{\max} \qquad (1)$$

$\kappa_{\max}$ is the biggest curvature constraint of planning path.

$$\kappa(t)=\frac{\left|r'(t)\times r''(t)\right|}{\left|r'(t)\right|^3}$$

(2) Torsion constraint

$$\left|\tau(t)\right|\le\tau_{\max} \qquad (2)$$

$\tau_{\max}$ is the biggest torsion constraint of planning path,

$$\tau(t)=\frac{\left[r'(t)\times r''(t)\right]\cdot r'''(t)}{\left|r'(t)\times r''(t)\right|^2}$$

(3) Climbing angle constraint

$$\left|\theta(t)\right|\le\theta_{\max} \qquad (3)$$

Among them, $\left|\theta(t)\right|=\tan^{-1}(\frac{z'(t)}{\sqrt{x'(t)^2+y'(t)^2}})$ and $\theta_{\max}$ is the biggest climbing angle constraint of UAV.

Farouki[18] points out that the curvature changes smoothly which the curve has the minimum energy and the planning path can be tracked easily. The bending energy, length of path, curvature constraint, torsion constraint and climbing angle constraint of planning path can be considered at the time of planning online. The calculation formula of performance index is given below.

(1) Considering climbing angle, the bending energy of path can be expressed as

$$\omega=\sqrt{\left(\frac{k(t)}{k_{\max}}\right)^2+\left(\frac{\tau(t)}{\tau_{\max}}\right)^2+\left(\frac{\theta(t)}{\theta_{\max}}\right)^2} \qquad (4)$$

In order to simplify the calculation, the literature [9] simplifies equation (4) into the form of equation (5).

$$\omega=\left|\theta(t)\right| \qquad (5)$$

(2) Length of path

At the time of planning three-dimensional PH path, the appropriate polynomial $\sigma(t)$ is selected to satisfy $\sigma^2(t)=x'^2(t)+y'^2(t)+z'^2(t)$, so the accurate length $s(t)$ of path can be calculated based on the integral of polynomial $\sigma(t)$.

$$s(t)=\int_{t_0}^{t_1}\left|\sigma(t)\right|dt \qquad (6)$$

Among them, the length of path that changes uniformly along the path can be obtained from the uniform variation of t.

(3) Performance indicator

$$J = \min(\lambda_1 \times s + \lambda_2 \times \bar{\kappa}_{\max} + \lambda_3 \times \bar{\tau}_{\max} + \lambda_4 \times \bar{\theta}_{\max})$$

The performance indicator J consider the constraints of curvature, torsion, climbing angle and the length of path comprehensively, which can make re-planning path satisfy the requirements of performance indicator and can quickly reach the goal.

b. Generation of three-dimensional PH path

The spatial polynomial curve $r(t) = x(t)i + y(t)j + z(t)k$ can be expressed by the method of quaternion, and it is PH curve only when $r(t)$ meets the following form,

$$\frac{dr(t)}{dt} = A(t)iA^*(t) \qquad (7)$$

Among them, $A(t)$ is the polynomial of quaternion, that is $A(t) = u(t) + v(t)i + p(t)j + q(t)k$.

In order to define spatial PH curve, to consider quadratic Bezier polynomial

$$A(t) = A_0(1-t)^2 + A_1 \bullet 2(1-t)t + A_2 t^2 \qquad (8)$$

Its coefficients of quaternion are:

$$A_r = u_r + v_r i + p_r j + q_r k$$

Among them, $r = 0,1,2.$

So the rate $\sigma(t)$ of planning path can be get,

$$\sigma(t) = u^2(t) + v^2(t) + p^2(t) + q^2(t) \qquad (9)$$

According to the equation (9), the length of path can be accurately calculated by using the formula (6).

The relationship of 6 control points $P_0 \sim P_5$, which the generation of three-dimensional PH curve needs, is given in literature [8].

$$P_1 = P_0 + \frac{1}{5} A_0 i A_0^* \qquad (10)$$

$$P_2 = P_1 + \frac{1}{10}\left(A_0 i A_1^* + A_1 i A_0^*\right) \qquad (11)$$

$$P_3 = P_2 + \frac{1}{30}\left(A_0 i A_2^* + 4A_1 i A_1^* + A_2 i A_0^*\right) \qquad (12)$$

$$P_4 = P_3 + \frac{1}{10}\left(A_1 i A_2^* + A_2^* i A_0^*\right) \qquad (13)$$

$$P_5 = P_4 + \frac{1}{5} A_2 i A_2^* \qquad (14)$$

Among them, $P_0 = p_s = (x_s, y_s, z_s)$ is the starting point and $P_5 = p_f = (x_f, x_f, z_f)$ is the ending point.

The parameters in the formula (7) can be solved by solving Hermit interpolating problem. As long as getting the values of A_0, A_1 and A_2, the control points of quintic PH curve can be obtained from equation (10) - (14).

As the initial point's coordinates $P_0 = p_s = (x_s, y_s, z_s)$ and direction cosine (λ_s, μ_s, v_s) of tangential direction dp_s are known, the free variables A_0 and ζ_0 can be solved according to the formula (15).

$$A_0 = \sqrt{\frac{1}{2}(1+\lambda_s)|dp_s|} \cdot \left(-\sin\zeta_0 + \cos\zeta_0 i + \frac{\mu_s \cos\zeta_0 + v_s \sin\zeta_0}{1+\lambda_s} j + \frac{v_s \cos\zeta_0 - \mu_s \sin\zeta_0}{1+\lambda_s} k \right) (15)$$

As the ending point's coordinates $P_5 = p_f = (x_f, x_f, z_f)$ and direction cosine (λ_f, μ_f, v_f) of tangential direction dp_f are known, the free variables A_2 and ζ_2 can be solved according to the formula (16).

$$A_2 = \sqrt{\frac{1}{2}(1+\lambda_f)|dp_f|} \cdot \left(-\sin\zeta_2 + \cos\zeta_2 i + \frac{\mu_f \cos\zeta_0 + v_f \sin\zeta_2}{1+\lambda_f} j + \frac{v_f \cos\zeta_2 - \mu_f \sin\zeta_2}{1+\lambda_f} \right) (16)$$

According to the formula (17), A_1 can be solved.

$$A_1 = -\frac{1}{4}(\qquad) \sqrt{\frac{1}{4\sqrt{2}} 1+\lambda)|c|} \cdot (-\sin\zeta_1 + \cos\zeta_1 i + \frac{u\cos\zeta_1 + v\sin\zeta_1}{1+\lambda} j + \frac{v\cos\zeta_1 - u\sin\zeta_1}{1+\lambda} k) \quad (17)$$

Among them, the parameters (λ, μ, v) is the direction cosine of c, and ζ_1 is the free variable. c can be obtained from formulas (18)and(19).

$$(3A_0 + 4A_1 + 3A_2) i (3A_0 + 4A_1 + 3A_2)^* =$$

$$120(p_f - p_s) - 15(d_s + d_f) + 5\sqrt{(1+\lambda_s)|dp_s|(1+\lambda_f)|dp_f|}$$

$$\cdot \left[\begin{array}{l} \left[\cos(\zeta_2 - \zeta_0) - \frac{(\mu_s\mu_f - v_s v_f)\cos(\zeta_2 - \zeta_0) + (\mu_s v_f - \mu_s v_f)\sin(\zeta_2 - \zeta_0)}{(1+\lambda_s)(1+\lambda_f)} \right] i \\ + \left[\frac{\mu_s \cos(\zeta_2 - \zeta_0) - v_s \sin(\zeta_2 - \zeta_0)}{(1+\lambda_s)} + \frac{\mu_f \cos(\zeta_2 - \zeta_0) + v_f \sin(\zeta_2 - \zeta_0)}{(1+\lambda_f)} \right] j \\ + \left[\frac{v_s \cos(\zeta_2 - \zeta_0) + u_s \sin(\zeta_2 - \zeta_0)}{(1+\lambda_s)} + \frac{v_f \cos(\zeta_2 - \zeta_0) - u_f \sin(\zeta_2 - \zeta_0)}{(1+\lambda_f)} \right] k \end{array} \right] \qquad (18)$$

Abbreviated to:

$$(3A_0 + 4A_1 + 3A_2) i (3A_0 + 4A_1 + 3A_2)^* = c_x i + c_y j + c_z k \qquad (19)$$

A_0 , A_1 and A_2 can be obtained from the starting point P_0 and ending point P_5 . The values of P_1, P_2, P_3 and P_4 can be calculated according to the formulas (10) - (14), and then put them into the formula:

$$r(t)=\begin{bmatrix}1 & t & t^2 & t^3 & t^4 & t^5\end{bmatrix}\begin{bmatrix}1 & 0 & 0 & 0 & 0 & 0\\ -5 & 5 & 0 & 0 & 0 & 0\\ 10 & -20 & 10 & 0 & 0 & 0\\ -10 & 30 & -30 & 10 & 0 & 0\\ 5 & -20 & 30 & -20 & 5 & 0\\ -1 & 5 & -10 & 10 & -5 & 1\end{bmatrix}\begin{bmatrix}P_0\\ P_1\\ P_2\\ P_3\\ P_4\\ P_5\end{bmatrix} \tag{20}$$

That is, the PH curve can be solved.

c. Analysis of 3-d PH path planning

It can be seen, from the generating process of PH curve, that the generating path is determined by the coordinates of the starting and ending points (P_s, P_f) ,the tangents' direction angles $(\phi_s, \theta_\mathrm{s}, \phi_\mathrm{f}, \theta_\mathrm{f})$, the tangents' length $(\varepsilon_s, \varepsilon_f)$ and three free angles (ξ_0, ξ_1, ξ_2) .

$$dx_s = \varepsilon_s \cos\theta_s \cos\phi_s$$

$$dy_s = \varepsilon_s \cos\theta_s \sin\phi_s$$

$$dz_s = \varepsilon_s \sin\theta_s$$

$$\varepsilon_s = \sqrt{dx_s^2 + dy_s^2 + dz_s^2} \tag{21}$$

$$dx_s = x_1 - x_0$$

$$dy_s = y_1 - y_0$$

$$dz_s = z_1 - z_0$$

$$dx_f = \varepsilon_f \cos\theta_f \cos\phi_f$$

$$dy_f = \varepsilon_f \cos\theta_f \sin\phi_f$$

$$dz_f = \varepsilon_f \sin\theta_f$$

$$\varepsilon_f = \sqrt{dx_f^2 + dy_f^2 + dz_f^2} \tag{22}$$

$$dx_f = x_5 - x_4$$

$$dy_f = y_5 - y_4$$

$$dz_f = z_5 - z_4$$

Among them, (x_0, y_0, z_0), (x_1, y_1, z_1), (x_4, y_4, z_4) and (x_5, y_5, z_5) are the coordinates of control points of quintic PH curve respectively.

Through trial and error, it can obtain that the values of curvature, torsion and other performance index are smaller when ξ_1 takes smaller value, such as $\xi_1 = \frac{\pi}{30}$, and ξ_0, ξ_2 differ quite a bit, such as taking $\xi_0 = -\frac{\pi}{10}, \xi_2 = \frac{\pi}{10}$. In order to meet the requirements of UAV's curvature, torsion and climbing angle and so on performances, the start-stop tangents' length $(\varepsilon_s, \varepsilon_f)$ should be comprehensively considered with the location of starting and ending points, the start-end tangents' direction angles and so on.

In complex battlefield environment equipped with dynamic threats and so on, if the path needs to be re-planned according to sensors' information, so the insertion point and speed direction of a new path can be given, and then the optimizing generated method of path in this paper can be used for re-planning path quickly under the conditions of new path's start-end points.

(1) Influence of the values of $\varepsilon_s, \varepsilon_f$ on curvature, torsion

The starting point p_s and ending point p_f of UAV are set as (0, 0, 0) and (50, 20, 50), The starting angle and ending angle are set as $(\phi_s$, and $(\phi_f$, , and the biggest constraints of path's curvature and torsion are $k_{\max} = \pm\frac{1}{3}$ and $\tau_{\max} = \pm\frac{1}{3}$.

The starting climb-angle θ_s changes in step 10° within its scope $\left[-\frac{\pi}{2}, \right.$, and the other three angles remain unchanged. In case that the tangent vector's length ε_f of ending position is 20, 40 respectively, ε_s changes in step 20 within its scope $(20,100)$, the maximum curvature and torsion of each path are shown in figure 2, figure 3. The initial tangent vector's length ε_s is taken as 20, 40 respectively, ε_f changes in step 20 within its scope $(20,100)$, the simulation results are shown in figure 4, figure 5, and the curves in figure are conducted the truncation processing if curvature and torsion are greater than 1. The increasing of $\varepsilon_s, \varepsilon_f$ makes the path more easily meet the requirements of curvature and torsion.

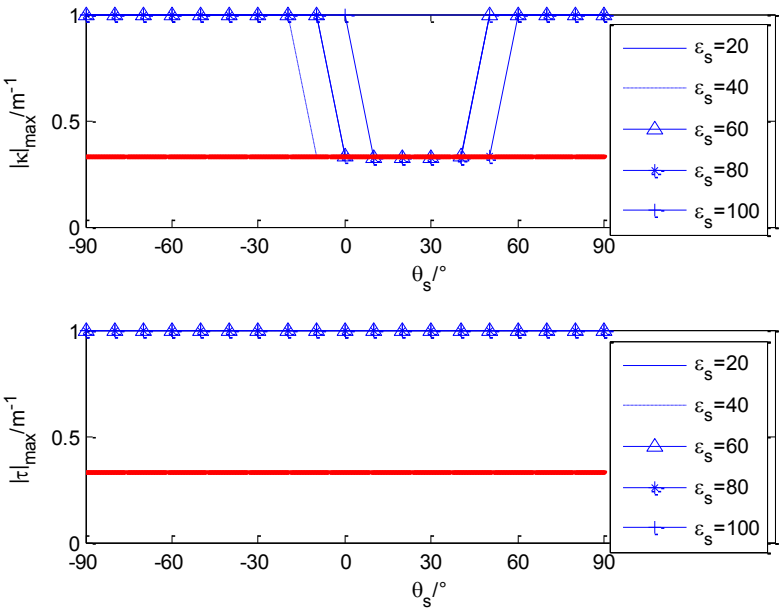

Figure 2. Path Maximum Curvature and Torsion Curve Varying with θ_s when $\varepsilon_f = 20$, ε_s Change at the Step 20

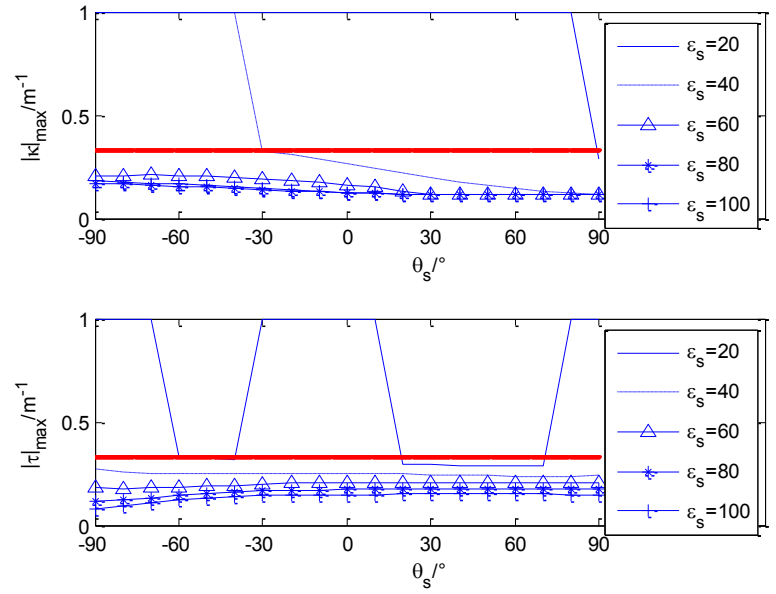

Figure 3 Path Maximum Curvature and Torsion Curve Varying with θ_s when $\varepsilon_f = 40$, ε_s Change at the Step 20

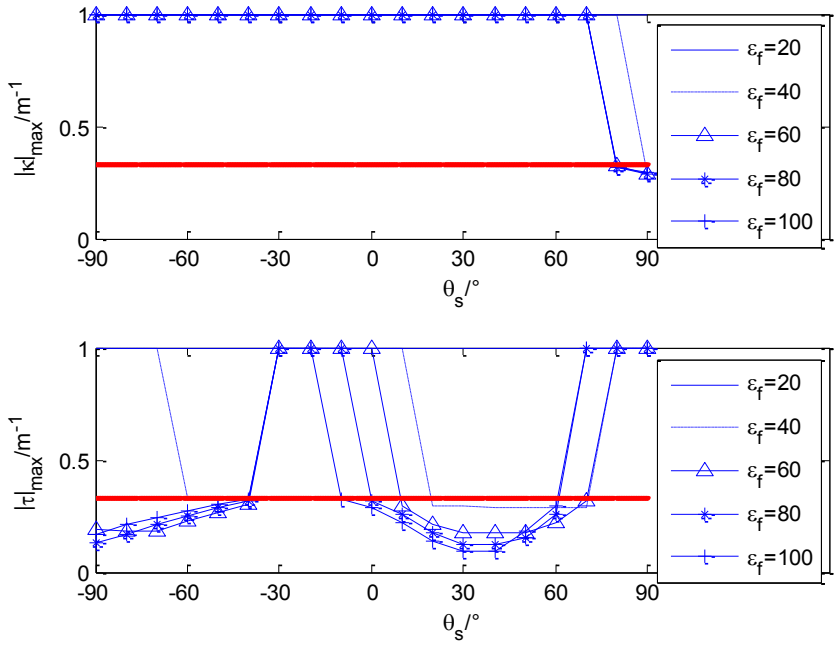

Figure 4 Path Maximum Curvature and Torsion Curve Varying with θ_s when $\varepsilon_s = 20$, ε_f Change at the Step 20

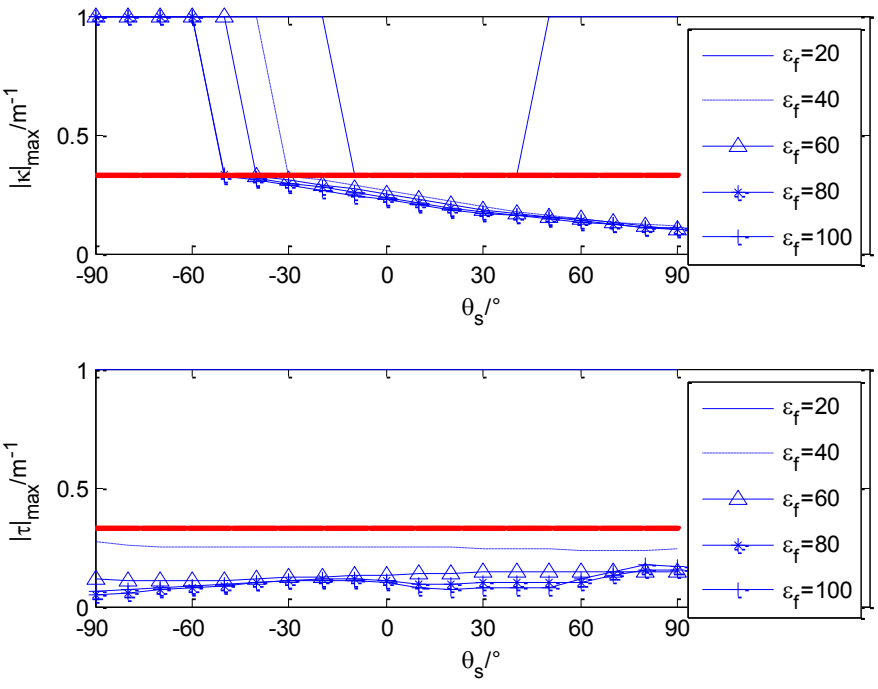

Figure 5 Path Maximum Curvature and Torsion Curve Varying with θ_s when $\varepsilon_s = 40$, ε_f Change at the Step 20

(2) Influence of the values of ε_s, ε_f on climbing angle

Under determining initial planning conditions, the relationship between climbing angle θ and ε_s, ε_f of planning path is given in Figure 5 to figure 8, among them, the horizontal coordinate is the path's length s. The tangent vector's length ε_f of ending position is 100, ε_s changes in step 100 within its scope $(400,1000)$, the biggest climbing angles of each path are shown in figure 6. The initial tangent vector's length ε_s is taken as 900, ε_f changes in step 50 within its scope $(50,350)$, the simulation results are shown in figure 7. From the figures, it can be seen that the increasing of ε_s, ε_f reduces the path's climbing angle, but the length of path will be increased.

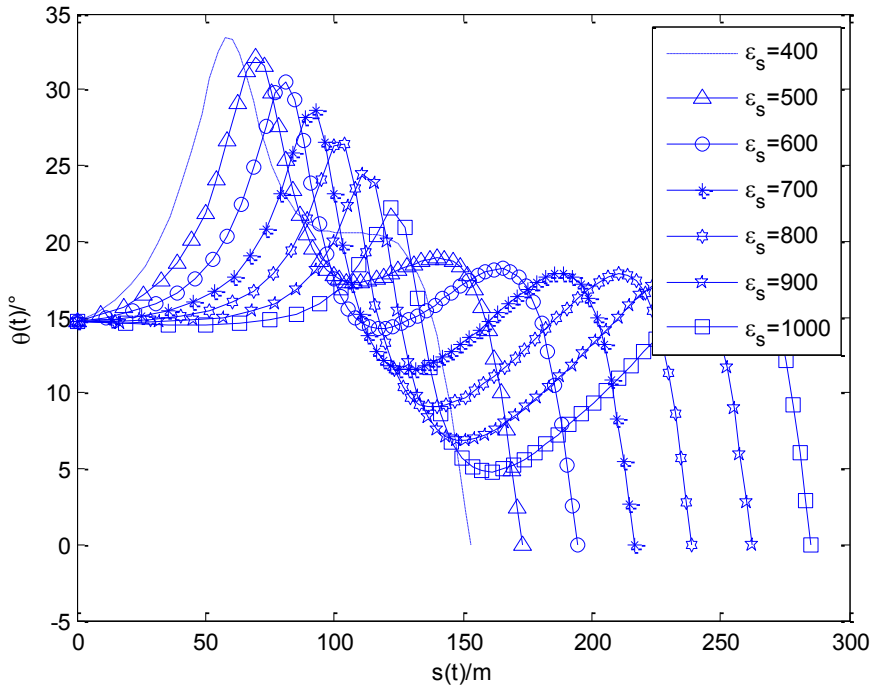

Figure 6. Path Climb Angle Curve Varying with θ_s when $\varepsilon_f = 100$, ε_s Change at the Step 100

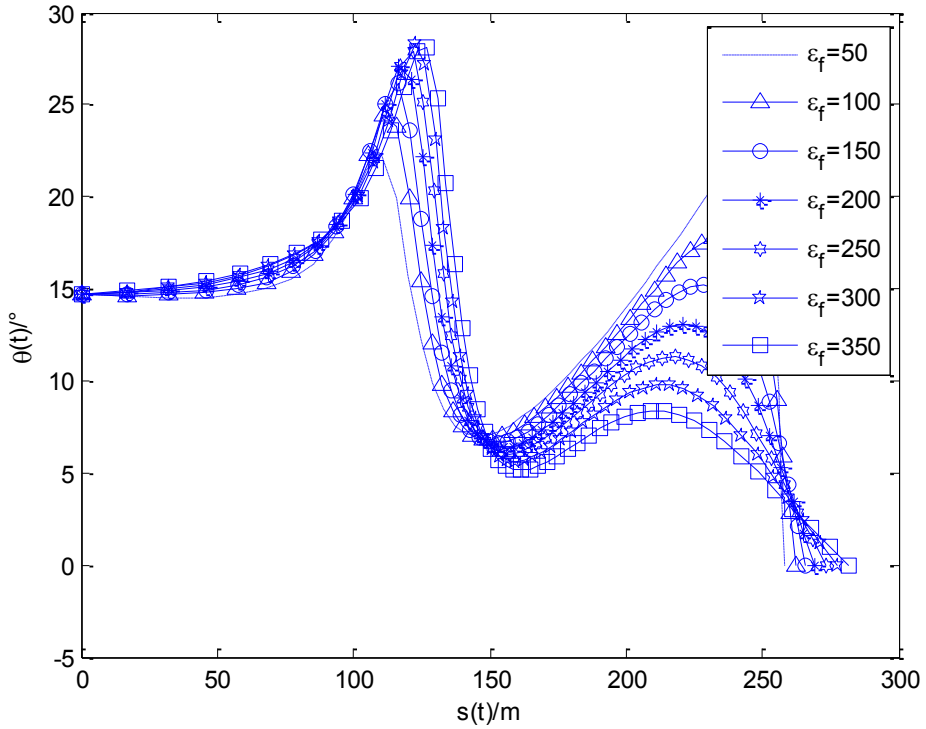

Figure 7. Path Climb Angle θ Curve when $\varepsilon_s = 900$, ε_f Change at the Step 50

Based on the above analysis, it can be seen that the flyable path, which satisfies the constraints of curvature, torsion and climbing angle, can be generated by increasing the values of ε_s, ε_f, but the length of planning path increases with the increasing of ε_s, ε_f. At present, the iteration method and try method are widely used for satisfying the requirements of the system's performance in literatures[7, 8]. At the same time, the way that the values of ε_s, ε_f increase at the same time[9] ignores the coordinating role between them.

In order to solve the above problem, the ranges of parameters' values that satisfy system's performance constraints are given below, and the method of quick path planning that meets the requirements of performance indexes is obtained by using Estimation of Distribution Algorithms.

III. OPTIMIZATION AND GENERATION OF PATH

Estimation of Distribution Algorithms establishes mathematical model for the whole group and adopts the probability estimation model to describe the evolution trend of the entire group directly. It establishes mathematical model of biological evolution in the "macro" level, which has good global search ability, and it doesn't necessarily use crossover operation of genetic algorithm and so on. So it evolves rapidly and it is suitable for the optimization problems which

have less number of variables. Besides, it can adopt the way of interval selection, and it is especially suitable for the situation that the feasible value ranges of ε_s , ε_f ,which meet the dynamic performance constraints, firstly need to be found out in this paper, and then do optimization. So the algorithm is proposed that Estimation of Distribution Algorithms is used to conduct optimization of path's parameters.

a. Determination on genes' value scopes

Based on the values of ε_s , ε_f , the individual genes in Estimation of Distribution Algorithms can be encoded. In order to speed up the optimization, the reasonable value ranges of each gene are given.

(1)Determination on value scopes of ε_s , ε_f that meet the constraints of torsion and curvature

Considering different initial angles and terminational angles and not considering climbing angle firstly, to analysis the maximum values of curvature and torsion under the condition that tangent vectors' length ε_s , ε_f take different values.

The shortest Dubins path's distance from the initial point to termination point can be written as $\left|p_s p_f\right|$. The tangent vectors' length are set as:

$$\varepsilon_f = \frac{1}{3}\left|p_s p_f\right| \qquad (23)$$

$$\varepsilon_s = \frac{1}{3}\left|p_s p_f\right| \qquad (24)$$

Through simulations, it found that the values of tangent vectors' angle take over the whole scope, but the curvature and torsion still can not meet the conditions ($-1/3 \le \kappa \le 1/3$, $-1/3 \le \tau \le 1/3$), the calculation results are shown in table 1.

Table 1: The Path Maximum Curvature and Torsion at Different Initial Angle with ε_s、 equal to $\frac{1}{3}\left|p_s p_f\right|$

Performance index (ϕ_s, , ,)	$\left\|\bar{\kappa}(t)\right\|_{\max}$	$\left\|\bar{\tau}(t)\right\|_{\max}$
($-\frac{\pi}{2}$, , ,)	**0.679**	**0.727**
($-\frac{\pi}{2}$, , ,)	**0.716**	**0.671**

$(-\frac{\pi}{2}, \frac{\pi}{6}, \frac{\pi}{4})$	**0.664**	**0.628**
$(-\frac{\pi}{2}, \frac{\pi}{4})$	**0.558**	**0.586**
$(-\frac{\pi}{2}, \frac{\pi}{6}, \frac{\pi}{4})$	**0.421**	**0.547**
$(-\frac{\pi}{2}, \frac{\pi}{3}, \frac{\pi}{4})$	**0.332**	**0.522**
$(-\frac{\pi}{2}, \frac{\pi}{2}, \frac{\pi}{4})$	**0.255**	**0.522**

Under the condition that the tangent vectors' length are equal to $\frac{1}{2}|p_s p_f|$, the calculation results of the path' maximum curvature $|\bar{\kappa}(t)|_{\max}$ and torsion $|\bar{\tau}(t)|_{\max}$ are shown in table 2. At this time, the path that does not meet the constraints still has a lot.

Table 2: The Path Maximum Curvature and Torsion at Different Initial Angle with ε_s、 equal to $\frac{1}{2}|p_s p_f|$

Performance index / $(\phi_s, \ , \ , \ )$	$|\bar{\kappa}(t)|_{\max}$	$|\bar{\tau}(t)|_{\max}$
$(-\frac{\pi}{2}, \frac{\pi}{4}, \frac{\pi}{4})$	**0.375**	**0.331**
$(-\frac{\pi}{2}, \frac{\pi}{3}, \frac{\pi}{4})$	**0.395**	**0.303**
$(-\frac{\pi}{2}, \frac{\pi}{6}, \frac{\pi}{4})$	**0.365**	**0.297**
$(-\frac{\pi}{2}, \frac{\pi}{4})$	**0.304**	**0.292**
$(-\frac{\pi}{2}, \frac{\pi}{6}, \frac{\pi}{4})$	**0.224**	**0.283**
$(-\frac{\pi}{2}, \frac{\pi}{3}, \frac{\pi}{4})$	**0.171**	**0.274**
$(-\frac{\pi}{2}, \frac{\pi}{2}, \frac{\pi}{4})$	**0.375**	**0.331**

The tangent vectors' length are equal to $\frac{2}{3}|p_s p_f|$, the calculation results of the path' maximum curvature $|\bar{\kappa}(t)|_{\max}$ and torsion $|\bar{\tau}(t)|_{\max}$ are shown in table 3. At this time, the planning path can satisfy the constraints in most cases.

Table 3: The Path Maximum Curvature and Torsion at Different Initial Angle with ε_s、 equal to $\frac{2}{3}\left|p_s p_f\right|$

Performance index (ϕ_s, , ,)	$\left\|\bar{\kappa}(t)\right\|_{\max}$	$\left\|\bar{\tau}(t)\right\|_{\max}$
($-\frac{\pi}{2}$, $\frac{\pi}{4}$, $\frac{\pi}{4}$)	**0.264**	**0.146**
($-\frac{\pi}{2}$, $\frac{\pi}{3}$, $\frac{\pi}{4}$)	**0.267**	**0.141**
($-\frac{\pi}{2}$, $\frac{\pi}{6}$, $\frac{\pi}{4}$)	**0.241**	**0.153**
($-\frac{\pi}{2}$, $\frac{\pi}{4}$)	**0.199**	**0.166**
($-\frac{\pi}{2}$, $\frac{\pi}{6}$, $\frac{\pi}{4}$)	**0.144**	**0.173**
($-\frac{\pi}{2}$, $\frac{\pi}{3}$, $\frac{\pi}{4}$)	**0.105**	**0.172**
($-\frac{\pi}{2}$, $\frac{\pi}{4}$, $\frac{\pi}{4}$)	**0.0927**	**0.174**

From the above analysis, the floor of $\varepsilon_s, \varepsilon_f$ can be taken as $\frac{1}{3}\left|p_s p_f\right|$.

(2) Determination on value scopes of $\varepsilon_s, \varepsilon_f$ that meet the constraints of climbing angle

In literature [9], the formula (5) is used to calculate the bending energy and formulas (25), (26) are adopted to do iteration of $\varepsilon_s, \varepsilon_f$, which make the planning path meet the constraint of climbing angle.

$$\varepsilon_s = \varepsilon_s + \left(\frac{\varepsilon_0}{\varepsilon_0 + \varepsilon_5}\right)(\rho_{\min} + \sigma_{\min}) \quad (25)$$

$$\varepsilon_f = \varepsilon_f + \left(\frac{\varepsilon_5}{\varepsilon_0 + \varepsilon_5}\right)(\rho_{\min} + \sigma_{\min}) \quad (26)$$

Among them,

$$\varepsilon_0 = \int_0^{0.5} \omega(t)^2 \left|\bar{r}(t)\right| dt$$

$$\varepsilon_5 = \int_{0.5}^{1} \omega(t)^2 \left|\bar{r}(t)\right| dt$$

Algorithm can value that meets the constraints of system performance within finite steps, but large step causes that the length of planning path is longer than the other. Therefore, the iteration results of formulas (25) and (26) are regard as upper limit of ε_s , ε_f , which is regarded as heuristic information to reduce the number of iterations and improve planning performance in path's optimization and generation.

b. Establishment of interval probability estimation model

Estimation of Distribution Algorithms adopts probability estimation model to generate new species. The value ranges $[a_j, b_j]$ of each variable $\boldsymbol{x}_j$ ($j = \{1,2,\ldots,M\}$, M is the number of genes) in individual X_i ($i = \{1,2,\ldots$,) are divided into n equidistant sections, it chooses elite individuals with probability p_e in the generated species, and calculates the probability p_{jk} ($k = \{1,2,\ldots,n\}$) in the kth interval $[a_{jk}, b_{jk}]$ of the jth dimension locus. At the time of generating a new individual, a random number p^j is randomly generated between (0, 1) for each gene, if $\sum_{k=1}^{s} p_{jk} < p^j \le \sum_{k=1}^{s+1} p_{jk}$ ($s = \{1,2,\ldots,n-1\}$), the values in $(s+1)th$ interval $[a_{js}, b_{js}]$ are selected to randomly generate new genes. And if $p^j \le p_{j1}$, the values in interval $[a_{j1}, b_{j1}]$ are selected to randomly generate new genes.

The interval probability estimation model based on elite individuals is adopted to make the excellent genes improve quickly in the next generation and speed up the process of evolution.

c. The optimization and generation step of three dimensional path based on Estimation of Distribution Algorithms

1) To determine the parameter values' range of initial and terminate tangent vectors, to encode gene with real number and divide the interval, to initialize the new species' individual;

2) To calculate the adaptive value J for the individuals that meets the constraints of dynamic performances, to choose the elite individuals with the probability p_e in the generated population, and to reserve the best individual;

3) To calculate the interval probability estimation model of each gene in population, and to generate new population based on this model;

4) To optimize in the neighborhood for the best individual X_b ; to stop evolving when the best individual's fitness value does not change in gth generation or reach the maximum evolution generation. Otherwise, to turn to step 2) and continue to evolve.

IV. PATH RE-PLANNING UNDER THREATEN ENVIRONMENT

If the UAV detects obstacles in flight, the position of the insertion point and angle direction for obstacle avoidance can be calculated. The optimally flyable PH path can be generated between real-time position in which the obstacles are detected and insertion point, insertion point and termination point respectively, which are used to change the original path. In order to ensure continuity of path, the tangent direction of the path remains unchanged in detection point and insertion point.

V. SIMULATION RESULTS AND ANALYSIS OF PATH PLANNING

a. The optimization and generation of PH path

The Estimation of Distribution Algorithms, which is proposed in this paper, is used to perform simulation experiment on the three-dimensional PH path planning problem. For this simulation, the initial and final positions of the UAV, the derivatives at these positions, the kinematic constraints are summarized in table 1.

Table 1. Simulation Conditions Setting of UAV

Initial Pose			**Final Pose**			**Detection distance** (m)	**Kinematic Constraints** $\kappa_{\max}$ $\tau_{\max}$	*Climbing angle* Constraint
Position	*Derivatives*		*Position*	*Derivatives*				
	Heaing angle	*Climbing angle*		*Heading angle*	*Climbing angle*			
(0,0,0)	$-\frac{\pi}{2}$	$\frac{\pi}{12}$	(50,20,50)	$\frac{\pi}{2}$	0	100	±0.33 ±0.33	$\frac{\pi}{6}$

The selection probability of elite individual is taken as $p_e = \frac{1}{3}$ in Estimation of Distribution Algorithms. When the simulation contains climbing angle constraint, the minimum values of ε_s, ε_f can be found by the iterative method in literature [9], which satisfy three constraints. The simulation results are shown from figure 8 to figure 10. And it can get $\varepsilon_s = 942.4907$, $\varepsilon_f = 289.5093$, $|\bar{\kappa}|_{\max} = 0.233$, $|\bar{\tau}|_{\max} = 0.045$, $s = 286.1$ and the number of iterations $i = 206$.

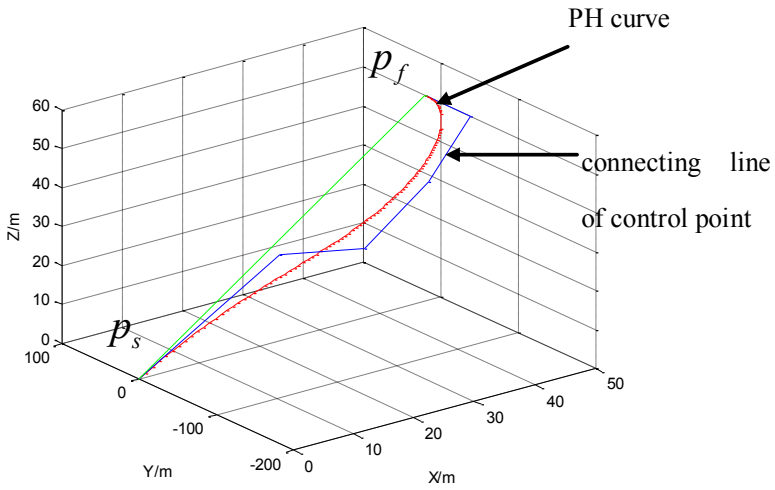

Figure 8. Path Curve Using Iteration Considering Climb Angle

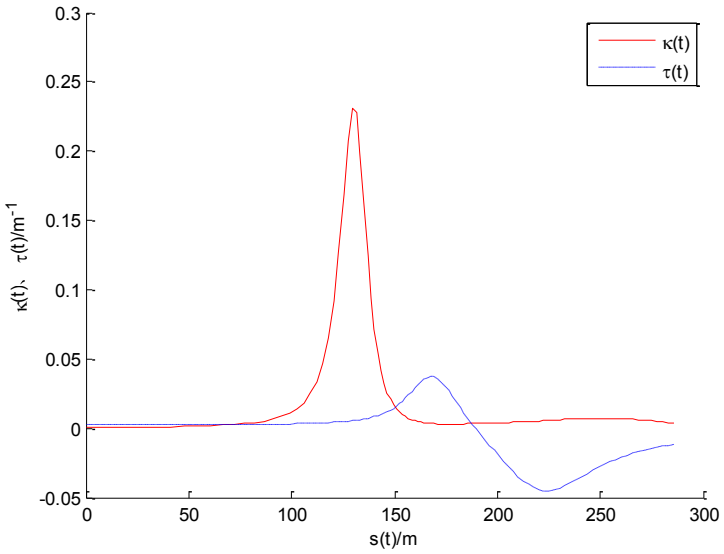

Figure 9. Curvature and Torsion Change with the Length of the Pathes in Figure 8

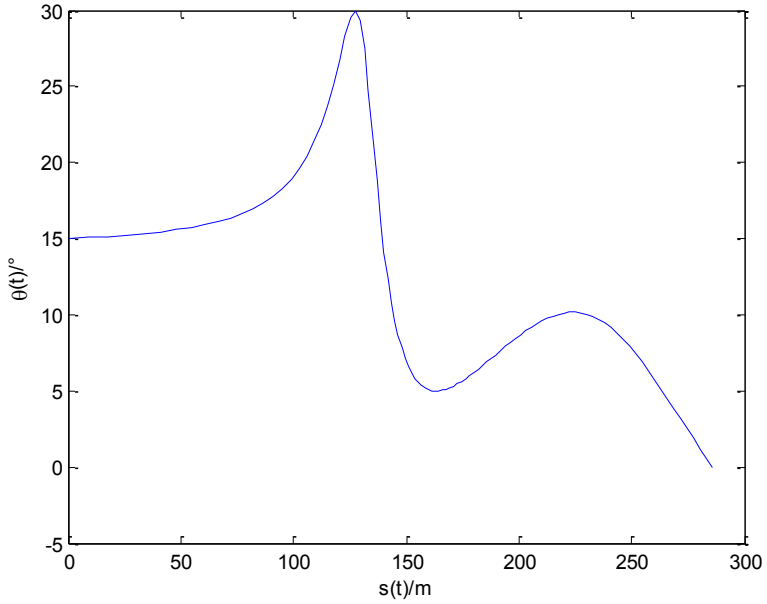

Figure 10. Climb Angle Change with the Length of the Path in Fig.8

The values of ε_s , ε_f , which are obtained by iteration, are regard as the upper limit, and $\frac{1}{3}\left|p_s p_f\right|$ is taken as the floor at the same time. The size of population is set as N=50, and evolutional generation is G=10. The parameters that correspond to the optimal value are $\varepsilon_s = 807.3519$, $\varepsilon_f = 114.7029$, $\left|\bar{\kappa}\right|_{\max} = 0.208$, $\left|\bar{\tau}\right|_{\max} = 0.234$, $\theta_{\max} = 29.2451^{\circ}$, $s = 242.0$. The parameters are set as $\lambda_1 = 0.001$, $\lambda_2 = 1$, $\lambda_3 = 1$, $\lambda_4 = 0.01$ at the time of calculating the performance index J .

When N=10, G=4, The parameters that correspond to the optimal value are $\varepsilon_s = 881.6855$, $\varepsilon_f = 197.5181$, $\left|\bar{\kappa}\right|_{\max} = 0.226$, $\left|\bar{\tau}\right|_{\max} = 0.0407$, $\theta_{\max} = 29.865^{\circ}$, $s = 245.2$. The generated path of last generation, which meets constraints, is shown in figure 11, and its curvature, torsion and climbing angle as shown in figure 12 and figure 13. The evolution curve of optimal individual's adaptive value in each generation is given in figure 14. Compared with the simulation results of N=50 , G=10, the algorithm has found a comparative optimal path, and its iteration number reduces a lot, which fully shows the rapidity of the algorithm. In comparison with the simulation results of figure 7-9, the method in this paper increase s few iterations compared with the paper [9], which can reduce the generated path's length a lot gives full consideration to the constraints of system performance.

The weight coefficients which contain the curvature, torsion, climbing angle and so on in performance index can be adjusted according to planning requirements. So when the path is re-planned, the insertion point of new path can be given, which makes UAV generate flyable path as soon as possible. And then UAV reaches the target point along the re-planning path.

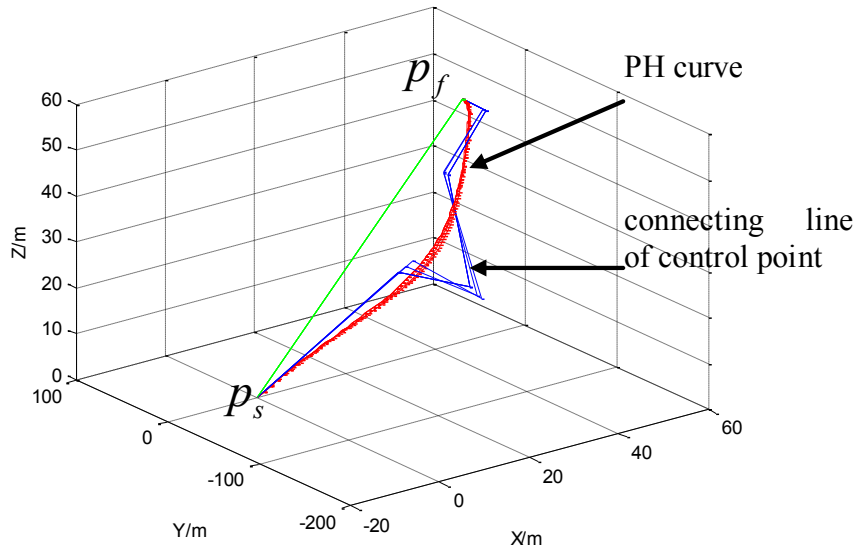

Figure 11. Pathes of the Last Generation Individual Considering Bounded Climb Angle

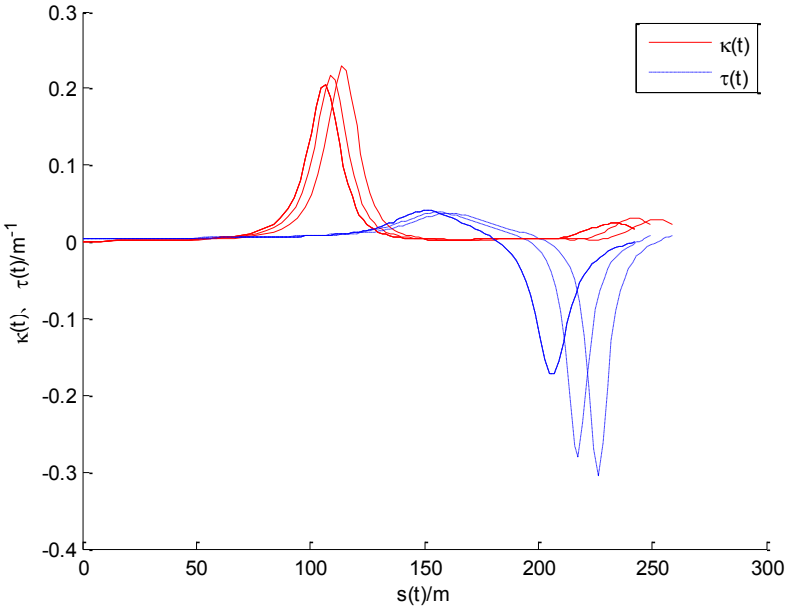

Figure 12. Curvature and Torsion Change with the Length of the Paths in Fig. 10

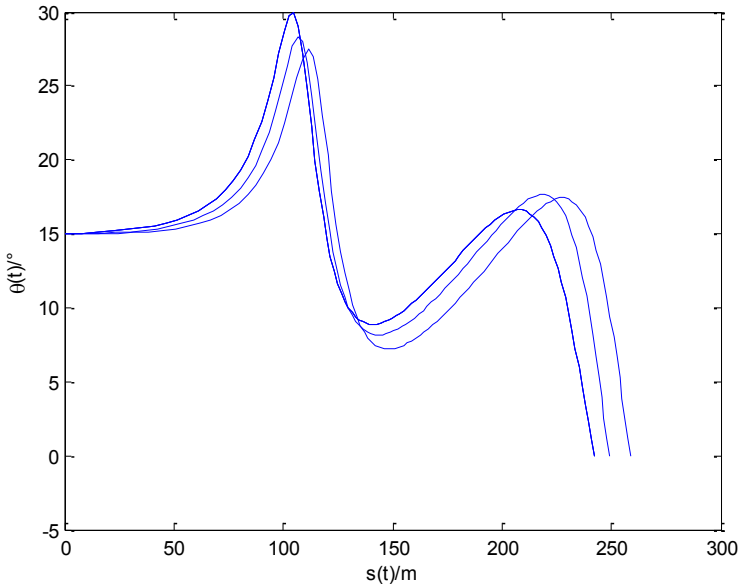

Figure 13. Climb Angle Change with the Length of the Pathes in Fig. 10

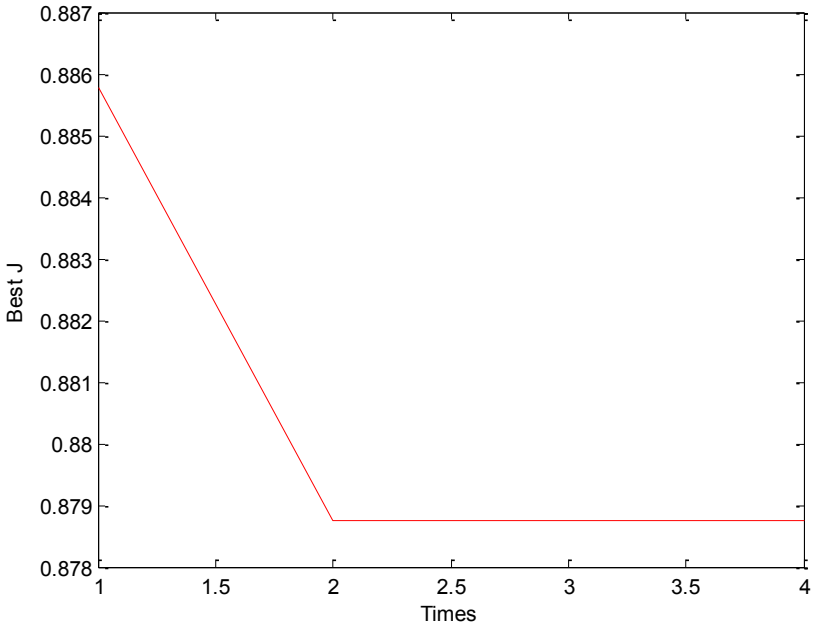

Figure 14. The Optimum Individual Fitness Evolution Curve

b. Obstacle avoidance path re-planning

For this simulation, the initial and final positions of the UAV, the derivatives at these positions, the kinematic constraints are summarized in table 2.

Table 2. Simulation Conditions Setting of UAV

Initial Pose		**Final Pose**		**Detection distance** (m)	**Kinematic Constraints**	**Velocity** (m/s)
Position	*Derivatives*	*Positio*	*Derivatives*			

	Heaing angle	*Climbing angle*	*n*	*Heading angle*	*Climbing angle*		$\kappa_{\max}$ $\tau_{\max}$	
(0,0,0)	60°	15°	(500,200,100)	0°	0°	100	±0.33 ±0.33	60

Suppose the UAV detect two moving obstacles at the point $\boldsymbol{P_u}(161.4,116.8,72.3)$, Obstacles position when UAV detect the obstacles, the velocity magnitude and direction of the obstacles, the radius of the obstacles are given in table 3.

Table 3. Simulation Conditions Setting of Obstacles

Obstacle	**Obstacle position**	**Velocity magnitude and direction**			**Obstacle Radius(s)**
		magnitude	*Heading angle*	*Climbing angle*	
Obstacle1	(252,159,100)	32	120°	22°	30
Obstacle2	(144,215,60)	45	-30°	15°	20

UAV needs to do obstacle avoidance for obstacles O_1 , O_2 by judgment. By calculation, the interruption point $\boldsymbol{Q}$ is $\begin{bmatrix} \hat{\boldsymbol{x}}_{\boldsymbol{u}} \\ \hat{\boldsymbol{y}}_{\boldsymbol{u}} \\ \hat{\boldsymbol{z}}_{\boldsymbol{u}} \end{bmatrix} = \begin{bmatrix} 170.5 \\ 199.9 \\ 83.0 \end{bmatrix}$. The two direction angles at the interruption points are $\phi_{\boldsymbol{u}} = 40.27^{\circ}, \theta_{\boldsymbol{u}} = 29.73^{\circ}$. The adjustment time from the detection point to the interruption point is $\boldsymbol{t_s} = 1.2$. After $\boldsymbol{t_s}$, the coordinates of $\boldsymbol{O}_1, \boldsymbol{O}_2$ are $\boldsymbol{O}_1'(233,190,50), \boldsymbol{O}_2'(191,187,75)$. The UAV rotated angle is $\alpha = 3.4^{\circ}$. The obstacle avoidance result that takes the horizontal plane as the plane of obstacle avoidance is given in Fig.15.

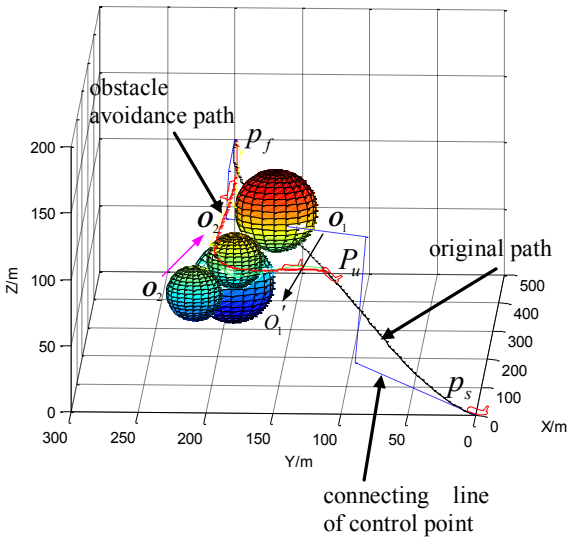

Figure 15. The Result of the obstacles Avoidance in horizontal plane

It can be seen from the simulation results that UAV successfully realize the obstacle avoidance. The horizontal or vertical plane can be selected as the plane of obstacle avoidance according to specific needs.

VI. CONCLUSION

Considering the curvature, torsion and climbing angle constraint and so on dynamic performances during UAV flights, the quantic PH curve is used to generated three dimensional path, and based on the UAV's current coordinates, speed, flight state and target point's coordinates, speed and so on information, the flyable path that is curvature continuous can be real-timely planned, which provides a kind of good practical and feasible method that can realize autonomous planning and quickly generate flyable path in the real-time dynamic environment for UAV.

VII. ACKNOWLEDGEMENTS

This research is supported by Aeronautical Science Foundation of China under Grant No20135584010.

REFERENCES

[1] Reberto Conde, David Alejo, Jose Antonio Cobano, et al. Conflict Detection and Resolution Method for Cooperationg Unmanned Aerial Vehicles[J]. J Intel Robot Syst, 2012,65: 495-505.

[2] Lugo Cardenas, I., Flores, G., Salazar, S., Lozano, R.. Dubins Path Generation for a Fixed Wing UAV[C]. 2014 International Conference on Unmanned Aircraft Systems, 2014: 339-346.

[3] R. Dai, John E. Cochran Jr. Path Planning for Multiple Unmanned Aerial Vehicles by Parameterized Corno-Spiral[C]. American Control Conference Hyatt Regency Riverfront St. Louis, MO, USA June 10-12, 2009.

[4] Ozgur Koray Sahingoz. Generation of Bezier Curve-Based Flyable Trajectories for Multi-UAV System with Paralled Genetic Algorithm[J]. Journal of Intelligent & Robotic Systems, 2014, 74(1-2):499-511.

[5] Lee Fowler1 and Jonathan Rogers , Bézier Curve Path Planning for Parafoil Terminal Guidance[C]. AIAA Aerodynamic Decelerator Systems (ADS) Conference 25-28 March 2013, Daytona Beach, Florida, AIAA 2013-1325.

[6] Armando Alves Neto, Douglas G. Macharet, Mario F. M. Campos. Feasible path planning for fixed-wing UAVs using seventh order Bézier curves[J]. Journal of the Brazilian Computer Society, 2013, 19(2):193–203.

[7] Mohammed Afzal Shah. Cooperative path planning and cooperative perception for UAVs swarm[D]. CRANFIELD UNIVERSITY. PhD Thesis, 2011.

[8] Armando A. Neto and Mario F. M. Campos. A Path Planning Algorithm for UAVs with Limited Climb Angle[C]. The 2009 IEEE/RSJ International Conference on Intelligent Robots and Systems. October 11-15, 2009 St Louis, USA:3894-3899.

[9] Armando Alves Neto, Douglas G. Macharet, Mario F. M. Campos. On the Generation of Trajectories for Multiple UAVs in Environments with Obstacles[J]. Journal of Intelligent and Robotic Systems, 2010, 57(1):123–141.

[10] Seunghan Lim, Hyochoong Bang. UAV guidance laws to arrival at desired position and time from desired direction[C]. 2011 11th International Conference on Control, Automation and Systems. Oct. 26-29, 2011 in KINTEX, Gyeonggi-do, Korea:299-304.

[11] Cheng Y H, Wang X S, Hao M L. An Estimation of distribution algorithm with diversity preservation[J]. Acta Electronica Sinica, 2010, 38(3): 591-597.

[12] F. Belkhouche and B. Bendjilali. Reactive Path Planning for 3-D Autonomous Vehicles[J]. IEEE Transactions on Control Systems Technology. Vol. 20, No. 1, JANUARY 2012.

[13] D. Alejo, J.A.Cobano, M.A.Trujillo, et al. The Speed Assignment Problem for Conflict Resolution In Aerial Robotics[C]. 2012 IEEE International Conference on Robotics and Automation, May 14-18,2012: 3919-3424.

[14] T. Lauderdale, Probabilistic conflict detection for robust detection and resolution[C]. Proc. AIAA Aviation Technol., Integr., Oper., Indianapolis, 2012: 1–12.

[15] Basheer, G.S.,Ahmad, M.S.,Tang, A.Y.C.: A Framework for Conflict Resolution in Multi-agent Systems[C]. ICCCI2013. LNCS, Springer, vol.8083, 2013:195-204

[16] Ghusoon Salim Basheer1, Mohd Sharifuddin Ahmad1, Alicia Y.C. Tang1, et.al. A Novel Conflict Resolution Strategy in Multi-agent Systems: Concept and Model[C]. Advanced Approaches to Intelligent Information and Database Systems, Studies in Computational Intelligence 551, 2014: 35-45